JPET Fast Forward. Published on November 21, 2003 as DOI:10.1124/jpet.103.059600

MAP KINASE AND CASPASE SIGNALING PATHWAYS ARE REQUIRED FOR $P2X_7$ RECEPTOR ($P2X_7R$) INDUCED PORE FORMATION IN HUMAN THP-1 CELLS

Diana L. Donnelly-Roberts*, Marian T. Namovic, Connie R. Faltynek

and Michael F. Jarvis

Neuroscience Research,

Global Pharmaceutical Research and Development

Abbott Laboratories, Abbott Park, IL, 60064-6123

Text pages: 45

Tables: 3

Figures: 9

References: 43

Words in Abstract: 249

Words in Introduction: 606

Words in Discussion: 1436

Key Words: $P2X_7$, macrophage, pore formation, MAP kinase

Abbreviations: human purinergic receptor, hP2XR; LPS, lipopolysaccahride; MAPK, mitogen activated protein kinase; phosphorylated p38 MAPK, pp38 MAPK MAPK; IP3, inositol 1, 4, 5 -triphosphosphate; Fluorometric Imaging Plate Reader, FLIPR.

Running Title: $P2X_7R$- Mediated Pore Formation

*To whom correspondences should be addressed: Abbott Laboratories, 100 Abbott Park Rd., Bldg. AP9A, Dept. R4PM, Abbott Park, IL 60064-6123.

Tel. (847) 938-1422; Fax. (847) 937-9195;

email: diana.l.donnelly-roberts@abbott.com.

Abstract

Brief activation of the ATP-sensitive $P2X_7$ receptor ($P2X_7R$) stimulates the maturation and release of IL-1β in macrophages, whereas prolonged agonist activation induces the formation of cytolytic pores in cell membranes. The present studies investigated potential down-stream mechanisms associated with native human $P2X_7R$ activation in lipopolysaccahride (LPS) and interferonγ (IFNγ) differentiated THP-1 cells. BzATP–induced pore formation (EC_{50} = 35 μM) was blocked by a selective $P2X_7R$ antagonist, KN-62, (IC_{50}= 44 nM) and by PPADS, (IC_{50}= 344 nM). KN-62 and PPADS also blocked BzATP-induced IL-1β release (EC_{50} = 617 μM) with IC_{50} values of 75 and 3500 nM, respectively. The selective p38 MAP kinase inhibitor, SB 202190, potently inhibited BzATP-induced pore formation (IC_{50} = 75 nM), but did not alter $P2X_7$ mediated calcium influx or IL-1β release. SB 202190 and KN62 also attenuated BzATP-mediated activation of phosphoryated p38 MAPK (pp38 MAPK). Two caspase inhibitors, YVAD and DEVD, attenuated both BzATP-induced pore formation and IL-1β release in a concentration-dependent fashion. Neither DEVD nor p38-MAPK inhibitors blocked cell membrane pore formation evoked by maitotoxin or by activation of human $P2X_{2a}$ receptors. These results indicate that $P2X_7R$ mediated pore formation results from a coordinated cascade involving both the p38-MAPK and caspase pathways that is distinct from other cytolytic pore forming mechanisms. In contrast, $P2X_7R$ mediated IL-1β release is dependent on caspase activity but not p38 MAPK. Taken together, these results support the hypothesis that down-stream cellular signaling mechanisms rather than channel dilation mediates cytolytic pore-formation following prolonged agonist activation which underlies $P2X_7$ receptors.

The $P2X_7R$ is an ATP-sensitive, ligand-gated ion channel that functions as a nonselective cation channel and, upon prolonged agonist exposure, leads to the formation of progressively enlarged cytolytic pores (~ 900 Da) on the cell surface (North, 2002). Currently, seven different P2X receptor subtypes have been molecularly defined and the $P2X_7R$ appears to be the most divergent member of this family in terms of molecular structure, pharmacology, and function (North 2002; Jacobson et al., 2002). Homomeric $P2X_7Rs$ contain a longer intracellular C terminus compared to other P2X receptors. This C terminus is composed of a hydrophobic domain, as well as putative interaction sites for LPS (Denlinger et al., 2001), SH_2 domains (Kim et al., 2001), and α-actin (Kim et al., 2001). $P2X_7R$ mediated pore formation is dependent on an intact C terminus and is inhibited in the presence of extracellular divalent cations (Rassendren et al., 1997). Unlike many other P2XRs, the $P2X_7R$ does not form functional heteromeric combinations with other P2X subunits (Torres et al., 1999).

The $P2X_7$ receptor is also distinguished pharmacologically from other P2X receptors by the fact that ATP has weak affinity (EC_{50} > 100 μM) for this receptor whereas 2,3-O-(4-benzoylbenzoyl)-ATP (BzATP) is approximately 30-fold more potent than ATP (Surprenant et al., 1996; Bianchi et al., 1999). $P2X_7Rs$ are uniquely expressed on macrophages, epidermal Langerhans cells and other antigen-presenting cells (Suprenant et al., 1996). Within the CNS, $P2X_7R$ expression has been reported on microglia (Ferrari et al., 1996), astrocytes, Schwann cells (Grafe et al., 2000), and presynaptic neuronal terminals in hippocampus and spinal cord (Duechars et al., 2001).

Another unique function of the $P2X_7R$ is its contribution to a variety of pro-inflammatory events including fusion of macrophages to form multinucleated giant cells (Falzoni et al., 1995). Activation of $P2X_7$ receptors stimulates the release of the pro-inflammatory cytokine, interleukin-Iβ (IL-1β) in immune cells (Surprenant et al., 1996). IL-1β is processed from a precursor to a mature form by the enzyme, caspase I. ATP has been shown to both time and dose-dependently induce the release of IL-1β from LPS primed THP-1 cells (Grahames et al., 1999). This ATP-induced cytokine release appears to be specifically modulated by $P2X_7Rs$ since IL-1β release can be blocked not only by the nonselective P2X antagonists, PPADS and oxidized ATP, but also by KN-62, which is a selective $P2X_7R$ antagonist (Grahames et al., 1999). It has also been shown that the release of IL-1β is independent of cytolysis and appears not to require $P2X_7$-mediated pore formation (Chessell et al., 2001). $P2X_7R$ activation also results in cell membrane blebbing (Ferrari et al., 1997a), and changes in cellular morphology, which eventually leads to cell death by both necrotic and apoptotic mechanisms (Ferrari et al., 1999).

The present study evaluates the signaling pathways that contribute to two of the hallmark functional consequences of $P2X_7R$ activation, pore formation and IL-1β release, in differentiated human THP-1 macrophage cells. By using pharmacologically selective inhibitors of intracellular signaling pathways, we show that $P2X_7R$-induced pore formation and IL-1β release are mediated via some common but also some distinct mechanistic pathways. The mechanism of $P2X_7R$-mediated pore formation was also compared to pore formation induced by non-$P2X_7Rs$ such as the $P2X_{2a}R$ (Khakh et al., 1999) or via a toxin from marine dinoflagellates, maiototxin (MTX; Schilling et al.,

1999a,Schilling et al., 1999b). The exact mechanism by which prolonged activation of the $P2X_7R$ leads to pore formation remains unknown. Both dilation of the channel or recruitment of ancillary cellular mechanisms has been proposed (North, 2002). The present data provides evidence that $P2X_7R$ mediated pore formation is likely mediated by intracellular events rather than simply from an agonist-induced conformational change intrinsic to the channel.

Materials and Methods

Materials: Cell culture medium and phosphate buffered saline, pH 7.4 were obtained from BRL Life Technologies (Grand Island, NY). BzATP, ATP, UTP, PPADS, Protease Inhibitor Cocktail and lipopolysaccahride (LPS) were obtained from Sigma (St. Louis, MO). Maitotoxin was purchased from Wako Chemicals (Richmond, VA). Fluo-4 AM was purchased from Teflabs (Austin, TX) and Yo-Pro-1 (4-[(3-methyl-2(3H)-benzoxazolylidene) methyl]-1[3-(trimethylammonio)propyl]-diiodide was purchased from Molecular Probes (Eugene, OR). PD 98059, U0126, U0124, SB 202190-HCl, SB 203580, SB 202474, PD169316, JNK I and JNK II inhibitors and control analogs, Caspase 1 inhibitor (YVAD), Caspase 3 inhibitor (DEVD) and Cathepsin B, a casapse negative control inhibitor, were obtained from Calbiochem (San Diego, CA). The synthetic peptide dynorphin A was obtained from Bachem. Human interferonγ (IFNγ) and the IL-1β ELISA kit were obtained from R & D Systems (Minneapolis, MN) or Pierce Endogen (Rockford, IL). KN-62 was purchased from Biomol (Plymouth Meeting, PA). ELISA kits for the measurement of p38 MAPK [pTpY180/182] and total p38 were purchased from Biosource International (Camarillo, CA).

Tissue Culture: Cells of the THP-1 monocytic cell line (American Type Culture Collection, Rockville, MD) were maintained in the log phase of growth in RPMI medium containing high glucose and 10% fetal calf serum (BRL, Grand Island, NY) according to established procedures (Humphrey and Dubyak, 1996). Fresh vials of frozen THP-1 cells were initiated for growth every eight weeks. To differentiate THP-1 cells into a macrophage phenotype, a final concentration of 25 ng/ml of LPS and 10 ng/ml of IFNγ

were added to the cells (Humphrey and Dubyak 1996) either for 3 hours for IL-1β release assays or overnight (16 hours) for pore formation studies. 1321N1 cells stably expressing the recombinant human $P2X_{2a}$ receptor were grown and used according to previously published protocols (Bianchi, et al, 1999; Lynch et al., 1999). For both the pore formation and IL-1β release assays, cell density and viability were routinely assessed prior to each experiment by trypan dye exclusion and cells were found to be >90% viable following differentiation.

Calcium Influx Assay: The Fluorometric Imaging Plate Reader (FLIPR, Molecular Devices, Sunnydale, CA) was used to measure agonist-induced Ca^{2+} influx using the calcium chelating dye Fluo-4 as previously described by Bianchi et al 1999 with the following modifications. One to two hours before the calcium flux assay, the differentiated THP-1cells were washed in dPBS using a conical tube and loaded with Fluo-4 AM (2.28 μM) in D-PBS prior to centrifugation onto poly-lysine-coated black-walled 96-well plates. Cells were then maintained in a dark environment at room temperature. Immediately before the assay, each plate was washed three times with 250 μl D-PBS per well in order to remove extracellular Fluo-4 AM. Two 50 μl additions of test compounds (prepared in D-PBS) were made to the cells during each experiment. The first compound addition was made following a 30 sec baseline determination. Test compounds were incubated for 3 min before the addition of BzATP (final concentration of 30 μM) followed by incubation for an additional three minutes. Fluorescence data were collected at 1 s and then at 5 s intervals throughout the course of each experiment. Data shown are based on the maximal fluorescence response expressed in arbitrary relative fluorescence units (Bianchi et al., 1999). Concentration-response

data were analyzed using GraphPad Prism (San Diego, CA); the EC_{50} or IC_{50} values were derived from a single curve fit to the mean data of n=6 in duplicates.

Yo-Pro Uptake Assay: Agonist-induced pore formation was also determined using the FLIPR by measuring cellular uptake of Yo-Pro (MW=629 daltons) in differentiated THP-1 cells with the modifications below. Differentiated THP-1 cells were rinsed once in PBS without Mg^{2+} or Ca^{2+} ions, which have been shown to inhibit pore formation (Michel et al., 1999). The Yo-Pro iodide dye (1mM in DMSO) was diluted to a final concentration of 2 μM in PBS (without Mg^{2+} or Ca^{2+}) and then placed on the cells immediately prior to agonist addition. After the addition of various agonist concentrations (0.001 – 100 μM), Yo-Pro dye uptake was observed in the FLIPR equipped with an Argon laser (wavelength = 488 nm) and a CCD camera. The exposure setting of the camera was 0.25 sec with an f-stop setting of 2. Unless otherwise indicated, data points from each experiment were collected over a 60 min period following exposure to appropriate concentrations of BzATP. The intensity of the fluorescence was captured by the CCD camera every 15 seconds for the first 10 minutes of agonist exposure, followed by every 20 seconds for an additional 50 minutes. For antagonist activity measurements, the maximal intensity was expressed as a percent of that induced by 50 μM BzATP (the EC_{70} value for agonist activation) and plotted against the concentration of compound to determine IC_{50} values. For each experiment, differentiated control cells were also measured over the 60 min time course to assess background levels of fluorescence. This non-specific background Yo-Pro uptake, averaging 6-10% of the maximum BzATP response (see Figure 1), was subtracted from the maximum BzATP-induced fluorescence.

For experiments measuring $P2X_{2a}R$-mediated pore formation, a dose response curve was generated for the agonist ATP under the same conditions used for the $P2X_7R$ Yo-Pro uptake assay. EC_{70} value was determined and used to examine antagonist effects. For maiototoxin (MTX)-mediated pore formation studies, various concentrations of MTX were examined under the conditions described above except that the buffer, D-PBS (Life Technologies, Rockville MD) contained 0.9 mM $CaCl_2$ and 0.5 mM $MgCl_2$, as the presence of extracellular divalent cations are required for MTX activity (Schilling et al., 1999a,Schilling et al., 1999b).

pp38 MAPK ELISA Measurements: Undifferentiated THP-1 cells were plated into a T75 flask at a density of 5 x 10^6 cells /ml / well. The day prior to the experiment, the cells were differentiated with 25 ng/ml LPS and 10 ng/ml IFNγ for 16 hours at 37^OC. In the presence of the differentiation media, the cells were incubated with inhibitors for 30 minutes at 37^OC followed by stimulation with 100 μM BzATP for an additional 60 min at 37^OC. Pelleted cell lysates were rinsed in PBS, repelleted, and flash-frozen. On the day of the ELISA, cell lysates were lyzed and protein extracted in a 10 mM Tris buffer, pH 7.4, containing: 100 mM NaCl, 1 mM EDTA, 1 mM EGTA, 1 mM NaF, 20 mM $Na_4P_2O_7$, 2 mM Na_3VO_4, 1% Triton X-100, 10% glycerol, 0.1% SDS, 0.5% deoxycholate, 1 mM PMSF and a 5% final concentration of a Protease Inhibitor Cocktail. Lysates were clarified by centrifugation at 13,000 rpm for 10 min at 4^OC prior to the detection of pp38 MAPK or total p38 MAPK activity using an ELISA, following the manufacturer's instructions.

IL-1β ELISA Measurements: Undifferentiated THP-1 cells were plated in 24-well plates at a density of 1 x 10^6 cells /ml / well. On the day of the experiment, cells

were differentiated with 25 ng/ml LPS and 10 ng/ml IFNγ for 3 hours at 37^{O}C. In the presence of the differentiation media, the cells were incubated with inhibitors for 30 minutes at 37^{O}C followed by a challenge with 1 mM BzATP for an additional 30 min at 37^{O}C. Supernatants were collected after a 5 min centrifugation in microfuge tubes and assayed for the presence of mature IL-1β by ELISA, following the manufacturer's instructions. For each experiment, differentiated control cells were also measured over the 60 min time course of the assay to assess background IL-1β accumulation. This non-specific background IL-1β release, typically averaged 3-8% of the maximum BzATP response, was subtracted from the maximum BzATP-induced release.

Results

BzATP-Mediated Yo-Pro Uptake in THP-1 Cells. Yo-Pro incorporation into differentiated THP-1 cells was detectable 15 minutes following the addition of BzATP (300 μM) and continued to increase over a 60 min period. These results are consistent with the effects previously described using cells expressing the stably transfected recombinant, human $P2X_7R$ (Rassendren et al., 1997). Exposure of differentiated THP-1 cells to BzATP for 60 min resulted in a 15-fold increase in fluorescence (Figure 1A and 1B). In contrast, ATP (at concentrations up to 1 mM) resulted in only a slight increase in Yo-Pro uptake and UTP (1 mM) was also inactive (Fig.2A). BzATP-mediated Yo-Pro uptake (EC_{50} value of 35 ± 7 μM, Figure 2A) was attenuated by pretreatment with the $P2X_7$ receptor antagonists KN-62 and PPADS (Humphreys et al., 1998). The IC_{50} values obtained for KN-62 and PPADS were 44 ± 2 nM and 334 ± 17 nM, respectively (Figure 2B).

Blockade of Pore Formation with MAPK Inhibitors. Differentiated THP-1 cells were pretreated with various MAPK inhibitors for 30 min prior to addition of 50 μM BzATP. SB 202190, a selective p38 MAPK inhibitor (Lee et al., 1994), potently inhibited BzATP-stimulated Yo-Pro uptake with an IC_{50} value of 75 ± 6 nM (Figure 3). Two other p38 MAPK inhibitors, PD 169316 and SB 203580, also blocked pore formation but with lower potencies than was observed for SB 202190 (Table I). SB 202474, which is structurally similar to SB 202190 but lacks p38 MAPK inhibitory activity (Lee et al., 1994), exhibited no effect on Yo-Pro uptake (Table 1). The inhibition of BzATP-induced pore formation by SB 202190 was not due to antagonism of the activation of the $P2X_7R$ by BzATP since SB 202190 had no significant effect in the $P2X_7R$ Ca^{2+} influx assay

(IC_{50} value >100 μM) using a 1321 astrocytoma cell line transfected with $hP2X_7R$ (Bianchi, et a., 1999). Using this same cell line for pore formation measurements, it was determined that SB 202190 had an IC_{50} value of 1500 ± 180 nM.

PD 98059, a MEK kinase inhibitor (Pang et al., 1995), exhibited only weak inhibition of $P2X_7R$ mediated pore formation (IC_{50} ~ 100 μM, Figure 3). In addition in the 1321 astrocytoma cell line transfected with $hP2X_7R$, PD 98059 (IC_{50} value >100 μM) did not significantly block pore formation. Another MEK kinase inhibitor U0126 (Pang et al., 1995) did not significantly inhibit BzATP-stimulated Yo-Pro uptake (Table I). In addition, 5-iodotubercidin, a potent inhibitor of the ERK2 and adenosine kinases (Fox et al., 1998), also had no effect on $P2X_7R$-mediated pore formation (Table I).

Inhibition of BzATP-Mediated pp38 MAPK Activation. Differentiation of THP-1 cells produced a significant increase in the level of pp38 MAPK relative to that observed for undifferentiated cells (Figure 4). The level of pp38 MAPK in differentiated THP-1 cells was further enhanced by exposure to 100 μM BzATP. BzATP-induced pp38 MAPK activation was significantly attenuated ($P<0.05$) by the p38 MAPK specific inhibitor 10 μM SB 202190 and not by the inert analog, 10 μM SB 247474. This BzATP-induced pp38 MAPK activation was also significantly attenuated ($P<0.05$) by the $P2X_7$ selective antagonist, KN62 (10 μM), to a level commiserate to that observed for differentiated control THP-1 cells. BzATP stimulation had no affect on the total p38 MAPK detected (data not shown).

Blockade of Pore Formation with Caspase Inhibitors. YVAD, a caspase I inhibitor, inhibited BzATP-evoked Yo-Pro uptake in a concentration-dependent fashion (IC_{50} value of 8 ± 0.8 μM) (Figure 5). DEVD, a caspase III inhibitor, was slightly more

potent in inhibiting BzATP-evoked Yo-Pro uptake with an IC_{50} value of 3.2 ± 0.3 μM (Figure 5). Cathepsin B, which serves as a negative control for caspase inhibitors, as well as two synthetic peptides, oxytocin and dynorphin A, which have comparable molecular weights to the caspase inhibitors and are linked to an inert, longer peptide chain to increase cell permeability (Garcia-Calvo et al, 1998) were also examined for pore-forming inhibitory activity. None of these controls exhibited any significant effect on BzATP-evoked Yo-Pro uptake (Table I).

Effects of Other Signaling Pathway Inhibitors on $P2X_7R$ Mediated Pore Formation. Inhibitors of other signaling pathways were also assessed for effects on BzATP-induced Yo-Pro uptake. As shown in Table II, pretreatment with thapsigargin (Won and Orth, 1995) or Xestospongin C (Gafni et al., 1997) had no effect on BzATP-mediated Yo-Pro uptake, suggesting that neither mobilization of Ca^{2+} from internal stores nor IP_3-mediated Ca^{2+} release are involved in pore formation (Table II). In contrast, three PKC selective inhibitors, Go-6976, Ro-31-7549 and Ro-31-8220 exhibited concentration-dependent inhibition of BzATP-evoked Yo-Pro uptake with IC_{50} values of 4.8 μM, 2.5 μM and 2.4 μM, respectively (Table II). Two of these PKC inhibitors, Ro-31-7549 and Ro-31-8220, were equally effective in blocking $P2X_7R$ mediated calcium influx with IC_{50} values of 5.2 ± 0.5 μM and 3.5 ± 0.4 μM, respectively.

Inhibition of BzATP-Mediated IL-1β Release. BzATP evoked a concentration dependent increase in IL-1β release from differentiated THP-1 cells with an EC_{50} value of 617 ± 57 μM (Figure 6A). As shown in Figure 5B, the selective $P2X_7R$ antagonist, KN-62, potently blocked the BzATP-mediated release of IL-1β with an IC_{50} value of 66 ± 3 nM. The nonselective P2XR antagonist, PPADS also inhibited $P2X_7R$ mediated IL-1β

JPET Fast Forward. Published on November 21, 2003 as DOI: 10.1124/jpet.103.059600
This article has not been copyedited and formatted. The final version may differ from this version.

release with an IC_{50} value of 5.8 ± 0.35 μM (Figure 6B). BzATP-stimulated IL-1β release was not significantly inhibited by various MAPK inhibitors at concentrations up to 10 μM (Figure 7). In contrast, both caspase inhibitors, YVAD and DEVD, inhibited the BzATP-induced IL-1β release (Figure 7). Concentration-response determinations for the caspase 1 inhibitor, YVAD, and the caspase 3 inhibitor, DEVD yielded IC_{50} values of 9 ± 1 μM and 23 ± 3 μM, respectively (Figure 8). Two of the PKC inhibitors, Ro-31-7549 and Ro-31-8220, also blocked $P2X_7R$ mediated IL-1β release with IC_{50} values of 2.8 ± 0.6 μM and 5.0 ± 0.5 μM, respectively.

Non-$P2X_7$-Mediated Pore Formation. MTX, which produces cytolytic membrane pores via a non-$P2X_7R$-related mechanism (Schilling, et al., 1999a), induced pore formation in differentiated THP-1 cells with an EC_{50} value of 6.8 ± 0.4 pM (Figure 9A). This effect was blocked by calmidazolium (Figure 9B; Table III) consistent with previous reports (Schilling et al., 1999a).

Prolonged agonist-evoked activation of the $P2X_2$ receptors can also lead to the formation of cell membrane pores (Khakh et al., 1999). In 1321N1 cells stably expressing the recombinant, human $P2X_{2a}$ receptor (Lynch et al., 1999), ATP induced Yo-Pro uptake with an EC_{50} value of 3 ± 0.1 μM (Figure 9C). This ATP-induced $P2X_{2a}$ pore formation was blocked by PPADS with an IC_{50} value of 477 ± 12 nM (Figure 9D; Table III).

Table III summarizes the effects of several antagonists and inhibitors on pore formation mediated by $P2X_7$ receptors as well as by other mechanisms. The nonselective P2X receptor antagonist, PPADS, potently blocked agonist-evoked Yo-Pro uptake mediated by activated $P2X_7$ and $P2X_{2a}$ receptors, but was ineffective in blocking

the effects of MTX. The $P2X_7$ receptor-selective antagonist, KN-62, only blocked $P2X_7$-mediated Yo-Pro uptake. Calmidazolium blocked MTX-induced pore formation (IC_{50} = 8 μM) consistent with previous reports (Schilling et al., 1999b), but had no effect on $P2X_7R$- and $P2X_{2a}R$- mediated Yo-Pro uptake. U73122, a PLC inhibitor (Smith et al., 1996), that has been shown to block MTX-mediated cell death (Estacion and Schilling, 2002), only blocked MTX-induced Yo-Pro uptake with an IC_{50} value of 1800 ± 400 nM.

The caspase III inhibitor, DEVD, significantly inhibited both $P2X_7$ and $P2X_{2a}$-mediated Yo-Pro uptake in a concentration-dependent fashion, but did not block the MTX-induced pore formation (Table III). Interestingly, SB 202190, the specific and potent p38 MAPK inhibitor, blocked $P2X_7$-mediated pore formation but had no effect on Yo-Pro uptake mediated through either $P2X_{2a}$ receptors or MTX treatment.

Discussion

In the present studies, we examined putative signaling mechanisms for two functional endpoints that are associated with $P2X_7R$ activation, agonist-evoked pore formation (Yo-Pro uptake) and IL-1β release. BzATP-stimulated Yo-Pro uptake provided a pharmacologically specific assay for native human $P2X_7R$ function on differentiated THP-1 cells based on the order of agonist (BzATP >> ATP and UTP) and antagonist (KN-62 >> PPADS) potency (North, 2002; Jacobson et al., 2002). Inhibition of BzATP evoked IL-1β release showed a similar order of antagonist block. While the precise signaling mechanisms governing each of these events is not completely understood, activation of $P2X_7Rs$ has been associated with a number of downstream pathways including phospholipase D (PLD) (Humphreys and Dubyak 1996), phospholipase A_2 (PLA_2), nuclear factor kappa B (NF-kappa B) (Aga et al., 2002; Ferrari et al., 1997b), pro-caspase I (Verhoef et al., 2003), and MAPK (Aga et al., 2002; Armstrong et al., 2002; Bradford and Soltoff 2002).

Agonist-evoked $P2X_7R$ pore formation is a property shared by other non-desensitizing P2XRs (e.g. $P2X_2$, $P2X_{2/3}$ and $P2X_4$), but the time course and pore size formed by these receptors differs from that observed for the $P2X_7R$ (Khakh et al., 1999; Virginio et al., 1999; North, 2002). MTX also induces pore formation via a non-$P2X_7R$-mediated mechanism (Schilling et al., 1999a,Schilling et al., 1999b). Both intrinsic $P2X_7R$ channel dilation and $P2X_7R$-dependent recruitment of accessory proteins have been proposed as candidate pore forming mechanisms (North, 2002). Data demonstrating that $P2X_7R$ pore formation is progressive, occurs in multiple cell types,

and has an identical pharmacology for the opening of the cation channel support the intrinsic receptor hypothesis.

The present data demonstrate that natively expressed human $P2X_7R$-mediated pore formation, in differentiated THP-1 cells, can be blocked by selective inhibitors of p38 MAPK and caspase activity. The present data also show that BzATP stimulated the activation of pp38 MAPK above the levels induced by THP-1 cell differentiation with LPS and IFNγ (Ono and Han, 2000). The p38 MAPK inhibitor, SB 202190, as well as the $P2X_7$ selective antagonist, KN62, both significantly attenuated the BzATP-mediated production of pp38 MAPK providing evidence for a direct interaction between $P2X_7R$ activation and the p38 MAPK pathway. The p38 MAPK-dependent pore formation was also demonstrated in 1321N1 cells expressing recombinant human $P2X_7Rs$. The differential potency of SB 202190 to block agonist-evoked pore formation in differentiated THP-1 cells and in the recombinant receptor cell line likely reflects differences in receptor expression as assessed by differences in agonist-evoked YO-PRO fluorescence (unpublished observations). This finding provides the first evidence that these downstream intracellular events play a role in $P2X_7R$ mediated pore formation. The involvement of the p38 MAPK pathway may be mechanistically selective for $P2X_7R$ mediated pore formation since inhibitors of this pathway were ineffective in blocking $P2X_7R$ mediated IL-1β release and did not alter pore formation mediated by MTX or by activation of $P2X_{2a}$ receptors. The present demonstration that BzATP-evoked Yo-Pro uptake is modulated by both MAPK and caspase inhibition, whereas BzATP-stimulated IL-1β release is sensitive to only caspase inhibition, is consistent with

previous work suggesting that these $P2X_7$ receptor mediated events are at least in part mechanistically distinct (Mackenzie et al., 2001; Schilling et al., 1999b).

MAPKs are a family of serine and threonine kinases that are activated by various external stimuli to regulate a variety of intracellular events (English and Cobb 2002). To date, there are three major signaling protein families involved in the MAPK cascades: ERK1/2, which is mainly involved in cellular growth and proliferation; JNK/SAPK, which is involved in cellular stress from ultraviolet irradiation, heat shock or exposure to inflammatory cytokines; and the newest member, p38 kinase, which is activated upon exposure to inflammatory cytokines, endotoxins or osmotic shock and often leads to apoptotic cell death (Su and Karin, 1996).

In contrast to the inhibitory effects of p38 MAPK inhibitors on BzATP-stimulated Yo-Pro uptake, no significant attenuation of BzATP-evoked pore formation was observed by inhibitors of MEK, ERK1/2, or by inhibitors of intracellular Ca^{2+} mobilization and IP_3-mediated-Ca^{2+} release. Cell permeable JNK I and JNK II inhibitors, as well as negative control (JNK-inactive) analogs were found to produce a nonspecific inhibition of BzATP-induced pore formation (unpublished observations), thus limiting a mechanistic interpretation of these findings. Inhibitors of PKC were moderately effective in reducing BzATP-stimulated pore formation, consistent with a recent report demonstrating that PKC activation may be upstream from activation of p38 MAPK in some pathways (Bradford and Soltoff 2002). However, representative PKC inhibitors are equally effective in blocking both Ca^{2+} influx and IL-1β release indicating that this pathway may not be unique to pore formation but more generally involved in events mediated by $P2X_7$ activation. Alternatively, it cannot be ruled out that the effects of PKC

and JNK inhibitors may be mediated simply by blocking $P2X_7R$ activation (i.e. receptor antagonism). Taken together, the present data suggest that a $P2X_7$-linked PKC-p38 kinase pathway is involved in the cytolytic effects of prolonged $P2X_7R$ activation in differentiated THP-1 cells. Supportive evidence for the involvement of p38 MAPK activity in $P2X_7R$-induced depression of mossy fiber synaptic activity has been previously reported (Armstrong et al., 2002).

Another pathway triggered by $P2X_7R$ activation is the caspase pathway. The caspases are a family of cysteine proteases involved in both apoptosis and cytokine release (Thornberry and Lazebnik, 1995). Caspase 1 is involved in the release of mature IL-1β from leaderless pro IL-1β whereas caspase 3 activity has been shown to be involved in $P2X_7$ receptor mediated apoptotic cell death (Perregaux et al., 2001). In the present studies, the Caspase 1 and 3 inhibitors, YVAD and DEVD, exhibited concentration-dependent inhibition of $P2X_7$ mediated IL-1β release and Yo-Pro uptake. Interestingly, these compounds showed inverted potency orders in blocking these two $P2X_7$ receptor-mediated events. The Caspase 1 inhibitor, YVAD, was more potent than the Caspase 3 inhibitor, DEVD, in attenuating BzATP-stimulated IL-1β release while the reverse was true for pore formation. These differences suggest some degree of mechanistic divergence in the generation of these two $P2X_7$ receptor mediated events. This idea is further supported by the inability of p38 MAPK inhibitors to attenuate $P2X_7R$-mediated IL-1β release, whereas they effectively block $P2X_7R$-mediated pore formation. It should be noted that this apparent difference in mechanism cannot be explained by potential differences in cell death due to differentiation conditions since similar levels of lactate dehydrogenase released were observed under both assay

conditions (unpublished observations). While it has previously been shown that $P2X_7R$-mediated SAPK-MAPK activity is independent of caspase 1 or caspase 3 activity (Humphreys et al., 2000), this does not rule out the possibility that the caspase isozymes may participate in $P2X_7R$ stimulated pore formation along a parallel pathway. These two events are also temporally differentiated since it has been shown that IL-1β containing microvesicle shedding occurs within seconds of $P2X_7R$ activation (Mackenzie et al., 2001) while $P2X_7R$-mediated pore formation requires minutes of agonist exposure.

It was of interest to further investigate whether the involvement of the MAPK and caspase pathways were unique to $P2X_7$-mediated pore formation or common to other pore formation mechanisms such as those caused by MTX (Schilling et al 1999a) or $P2X_{2a}R$ activation (Khakh et al., 1999). In contrast to the effects on $P2X_7R$-mediated pore formation, the p38 MAPK inhibitor, SB 202190, did not block pore formation induced by MTX or $P2X_{2a}R$ activation. Both $P2X_7R$- and $P2X_{2a}R$-induced pore formation was attenuated by the Caspase 3 inhibitor, DEVD, suggesting an apoptotic cell death mechanism induced by prolonged activation of both P2X receptors (Thornberry and Lazebnik 1995). While not sensitive to MAPK or caspase inhibition, MTX-induced pore formation was significantly attenuated by calmidazolium and U73122, a putative inhibitor of PLC (Estacion and Schilling 2002). Taken together, these data demonstrate that pore formation mediated by activation of $P2X_7R$ is mechanistically distinct from that produced by MTX or agonist activation of $P2X_{2a}Rs$.

In conclusion, the present data demonstrate that both p38 MAPK and caspase pathways are involved in $P2X_7R$-mediated pore formation whereas the caspase

pathway but not p38 MAPK is mechanistically linked to agonist-evoked IL-1β release. These data are consistent with other recent reports (MacKenzie et al., 2001; Verhoef et al., 2003) indicating that many of the functional sequelae engendered by $P2X_7R$ activation including IL-1β release, membrane blebbing, and pore formation may be mediated by parallel, rather than convergent intracellular signal transduction pathways. These data also demonstrate that the involvement of p38 MAPK in pore formation is specific to $P2X_7R$ and does not contribute to the pore-forming mechanisms associated with activation of $P2X_{2a}R$ or by exposure to MTX. Collectively, the data support the hypothesis that pore formation is a consequence of $P2X_7R$ activation but dependent on the involvement of down-stream signaling interactions due to the mechanistic difference between pore formation and channel opening.

References

Aga M, Johnson CJ, Hart AP, Guadarrama AG, Suresh, M, Svaren J, Bertics PJ and Darien BJ (2002) Modulation of monocyte signaling and pore formation in response to agonists of the nucleotide receptor $P2X_7$. *J Leukocyte Biology* **72**:222-232.

Armstrong JN, Brust TB, Lewis RG and MacViar BA (2002) Activation of Presynaptic P2X7-Like Receptors Depresses Mossy Fiber-CA3 Synaptic Transmission through p38 Mitogen-Activated Protein Kinase. *J Neuroscience* **22**:5938-5945.

Bianchi BR, Lynch KJ, Touma E, Niforatos W, Burgard EC, Alexander KM, Park HS, Yu H, Metzger R, Kowaluk E, Jarvis MF and van Biesen T (1999) Pharmacological characterization of recombinant human and rat P2X receptor subtypes. Eur J Pharmacol. **376**:127-138.

Bradford MD and Soltoff SP (2002) $P2X_7$ receptors activate protein kinase D and p42/p44 mitogen-activated protein kinase (MAPK) downstream of protein kinase C. *Biochem J*. **366**:745-755.

Chessell IP, Grahames CBA, Michel AD and Humphrey PPA (2001) Dynamics of P2X7 Receptor Pore Dilation: Pharmacological and Functional Consequences. *Drug Dev Res* **53**:60-65.

Denlinger LC, Fisette PL, Sommer JA, Watters JJ, Prabhu U, Dubyak GR, Proctor RA and Bertics PJ (2001) The nucleotide receptor $P2X_7$ contains multiple protein- and lipid-interaction motifs including a potential binding site for bacterial lipopolysaccharide. *J. Immuno*l **167**:1871-1876.

Duechars SA, Atkinson L, Brooke RE, Musa H, Milligan CJ, Batten TFC, Buckley NJ, Parson SH and Deuchars J (2001) Neuronal P2X7 Receptors Are Targeted to Presynaptic Terminals in the Central and Peripheral Nervous System. J Neuroscience **21**:7143-7152.

Estacion M and Schilling WP (2002) Blockade of Maitotoxin-Induced Oncotic Cell Death Reveals Zeiosis. *BMC Physiol* **2**: 2-14.

English JM and Cobb MH (2002) Pharmacological Inhibitors of MAPK pathways. *TiPS* **23**:40-45.

Falzoni S, Munerati M, Ferrai D, Spisani S, Moreti S and DiVirglio F (1995) The Purinergic P2Z Receptor of Human Macrophage Cells: Characterization and Possible Physiological Role. *J Clin Invest* **95**:1207-1216.

Ferrari D, Villalba M, Chiozzi P, Falzoni S, Ricciardi-Castagnoli P and DiVirgilio F (1996) Mouse microglia cells express a plasma membrane pore gated by extracellular ATP. *J. Immunol* **156**: 1531-1539.

Ferrari D, Chiozzi P, Falzoni S, Dal Susino M, Melchiorri L, Baricordi OR, and DiVirgilio F (1997a) Extracellular ATP Triggers IL-1β Release By Activating the Purinergic P2Z Receptor of Human Macrophages. *J. Immunol* **159**:1451-1458.

Ferrari D, Wesselborg S, Bauer M, and Schulze-Osthoff K (1997b) Extracellular ATP Activates Transcription Factor NF-[kappa]B through the P2Z Purinoreceptor by Selectively Targeting NF-[kappa]b p65. *J Cell Biol*. **139**:1635-43.

Ferrari D, Los M, Bauer MKA, Vandenabeele P, Wesselborg S and Schulze-Osthoff K (1999) P2Z Purinoreceptor ligation induces activation of caspases with distinct roles in apoptotic and necrotic alterations of cell death. *FEBS Letters* **447**:71-75.

Fox T, Coll JT, Xie X, Ford PJ, Germann, UA, Porter MD, Pazhanisamy S., Flemimg MA, Galullo V, Su MSS and Wilson KP (1998) A single amino acid substitution makes ERK2 susceptible to pyridinyl imidazole inhibitors of p38 MAP kinase. *Protein Science* **7**:2249-2255.

Gafni J, Munsch JA, Lam TH, Catlin MC, Costa LG, Molinski TF and Pessah IN (1997) Xestospongins: Potent Membrane Permeable Blockers of the Inositol 1,4,5-Trisphosphate Receptor. *Neuron* **19**: 723-733.

Garcia-Calvo M, Peterson EP, Leiting B, Ruel R, Nicholson DW and Thornberry NA (1998) Inhibition of Human Caspases by Peptide-based and Macromolecular Inhibitors. *J. Biol Chem* **273**: 32603-32613.

Grafe P, Mayer C and Irnich D (2000) P2 Nucleotide receptors in peripheral nerve trunk. *Drug. Dev. Res* **50**:19 (S12-02).

Grahames GBA, Michel AD, Chessell IP and Humpreys PPA (1999) Pharmacological characerization of ATP-and LPS-induced IL-1β release in human monoctyes. *Br.J.Pharmacol* 127:1915-1921.

Humphrey BD and Dubyak GR (1996) Induction of the P2z/P2X7 Nucleotide Receptor and Associated Phospholipase D Activity by Lipopolysaccharide and IFN-γ in the Human THP-1 Monocytic Cell Line. *J. Immunology* **157**:5627-37.

Humphreys BD, Virginio C, Surprenant A, Rice J and Dubyak GR (1998) Isoquinolines as Antagonists of the P2X7 Nucelotide Receptor: High Selectivity for the Human versus Rat Receptor. *Mol Pharmacol* **54**:22-32.

Humphreys BD, Rice J, Kertesy SB and Dubyak GR (2000) Stress-Activated Protein Kinase/JNK Activation and Apoptotic Induction by the Macrophage P2X7 Nucleotide Receptor. J Biol Chem **275**:26792-26798.

Jacobson KA, Jarvis MF and Williams M (2002) Perspective: Purine and Pyrimidine. (P2) Receptors as Drug Targets. *J.Med.Chem.* **45:** 4057-4093**.**

Kim M, Jiang LH, Wilson HL, North RA and Suprenant A (2001) Proteomic and functional evidence for a $P2X_7$ receptor signaling complex. *EMBO J* **20:**6347-6358.

Khakh BS, Bao XR, Labarca C and Lester HA (1999) Neuronal P2X Transmitter-Gated Cation Channels Change Their Ion Selectivity in Seconds. *Nature Neurosci* **2**: 322-330.

Lee JC, Laydon T, McDonnell PC, Gallagher TF, Kumar S, Green D, McNulty D, Blumenthal MJ, Heys JR, Landvatter SW, Strickler JE, McLaughlin MM, Siemens IR, Fisher SM, Livi GP, White JR, Adams JL and Young, PR (1994) A Protein Kinase Involved in the Regulation of Inflammatory Cytokine Biosynthesis. *Nature* **372**: 739-746.

Lynch KJ, Touma E, Niforatos W, Kage KL, Burgard EC, van Biessen T, Kowaluk EA, Jarvis MF (1999) Molecular and functional characterization of human P2X(2) receptors. *Mol. Pharmacol*. **56**: 1171-1181.

MacKenzie A, Wilson HL, Kiss-Tosh E, Dower SK, North RA and Surprenant A (2001) Rapid Secretion of Interleukin-1β by Microvesicle Shedding. *Immunity* **8**:825-835.

Michel AD, Chessel IP, and Humphrey PPA (1999) Ionic Effects on Human Recombinant $P2X_7$ Receptor Function. *N-S Arch Pharmacol* **359**:102-109.

North R. Alan (2002) Molecular Physiology of P2X Receptors. *Physiol Rev* **82**:1013-1067.

Ono K and Han, J (2000) The p38 signal transduction pathway: activation and function. *Cell Signal* **12 (1)**:1-13.

Pang L, Sawada T, Decker SJ and Saltiel AR (1995) Inhibition of MAP Kinase Kinase Blocks the Differentiation of PC-12 Cells Induced by Nerve Growth Factor. *J. Biol Chem* **270**: 13585-13588.

Perregaux DG, Labasi J, Laliberte R, Stam E, Solle M, Koller B, Griffiths R and Gabel CA (2001) Interleukin-1β Posttranslational Processong-Exploration of $P2X_7$ Receptor Involvement. *Drug Dev Res* **53**:83-90.

Rassendren F, Buell GN, Virginio C, Collo G, North RA and Surprenant A (1997) The Permeabilizing ATP Receptor, $P2X_7$. *J Biol Chem* **272**:5482-5486.

Schilling WP, Sinkins WG and Estacion M (1999a) Maitotoxin Activates a Nonselective cation channel and a P2Z/P2X7-like cytolytic pore in human skin fibroblasts. *American Physiol Soc* C755-C765.

Schilling WP, Wasylyna T, Dubyak, GR, Humphreys BD and Sinkins WG (1999b) Maitotoxin and P2Z/$P2X_7$ Purinergic Receptors Stimulation Activate a Common Cytolytic Pore. *American Physiol Soc* C766-C776.

Smith RJ, Justen JM, McNab AR, Rosenbloom CL, Steele AN, Detmers PA, Anderson DC and Manning AM (1996) U-73122: A Potent Inhibitor of Human Polymorphonuclear Neutrophil Adhesion on Biological Surfaces and Adhesion-Related Effector Functions. *J Pharmacol Exp Therap* **278**:320-329.

Su B and Karin M (1996) Mitogen-Activated Protein Kinase Casacades and Regulation of Gene Expression. Curr. Opin. Immunol. **8**: 402-411.

Suprenant A, Rassendren F, Kawashima E, North RA and Buell G (1996) The Cytolytic P2z Receptor for Extracellular ATP Identified as a P2X Receptor (P2X7). *Science* **272**: 735-738.

Thornberry NA and Lazebnik Y (1995) Caspases:Enemies Within. *Science* **267**:1312-1316.

Torres GE, Haines WR, Egan TM and Voight MM (1998) Co-expression of $P2X_1$ and $P2X_5$ receptor subunits reveals a novel ATP-gated ion channel. *Mol. Pharmacol* **54**:989-993.

Verhoef PA, Estacion M, Schilling W and Dubyak GR (2003) P2X7 Receptor-Dependent Blebbing and the Activation of Rho-Effector Kinases, Caspases, and IL-1β Release. *J. Immunol* **170**: 5728-5738.

Virginio C, MacKenzie A, North RA and Suprenant A (1999) Kinetics of cell lysis, dye uptake and permeability changes in cells expressing the rat P2X7 receptor. *J. Physio*l **519** (Pt.2): 335-46.

Won JGS and Orth DN (1995) Role of Inositol Trisphosphate-Sensitive Calcium Stores in the Regulation of Adrenocorticotropin Secretion by Perifused Rat Anterior Pituitary Cells. *Endocrinology* 136: 5399-5408.

Figure Legends

Figure 1. A. Kinetics of BzATP-stimulated Yo-Pro uptake in LPS/IFNγ treated (a) and untreated (b) human THP-1 cells. Traces represent responses from individual wells of confluent THP-1 cells. B. BzATP (300 μM) stimulated Yo-Pro uptake in LPS/IFNγ treated (gray bar) and untreated (black bar) human THP-1 cells Data represent means ± S.E.M. of 3-5 experiments.

Figure 2. A. Concentration-effect curves for P2 receptor agonists to stimulate Yo-Pro uptake in LPS/IFNγ differentiated THP-1 cells. Data were normalized to the peak BzATP response (% Maximum Response). B. Concentration-effect curves for $P2X_7R$ receptor antagonists to block BzATP (50 μM) stimulated Yo-Pro uptake. Data represent mean ± S.E.M. of 4-6 experiments.

Figure 3. Concentration-effect curves for two MAPK inhibitors, SB 202190 and PD 98059, to inhibit BzATP (50 μM)-induced Yo-Pro uptake. Data represent mean ± S.E.M. of 3-5 experiments.

Figure 4. Activation of pp38 MAPK in differentiated (16 hours) and non-differentiated (control) THP-1 cells. The BzATP (100 μM) induced pp38 MAPK activation was attenuated by SB202190 and KN62 and not by SB 247474. Data were normalized to the peak BzATP response of pp38 MAPK over total p38 (% Maximum Response), which ranged from 2000-3000 ng/ml of pp38 MAPK product. Data represent means ±

S.E.M. of 3 experiments. * P <0.05 vs. differentiated THP-1 cells and ** P<0.05 vs. BzATP treated differentiated THP-1 cells.

Figure 5. Concentration effect curves for a (A) caspase 1 inhibitor, YVAD and a (B) caspase 3 inhibitor, DEVD to attenuate BzATP (50 μM)-induced Yo-Pro uptake. Data represent mean ± S.E.M. of 3-5 experiments.

Figure 6. A. Concentration effect curve for BzATP stimulated release of mature IL-1β in LPS/IFNγ differentiated THP-1 cells. B. Concentration-dependent inhibition of BzATP (1 mM) stimulated IL-1β release by KN-62 and PPADS. Inhibition data were normalized to the peak BzATP response (% Maximum Response), which ranged from 200-600 pg/ml of IL-1β released. Data represent means ± S.E.M. of 3-5 experiments.

Figure 7. Effect of MAPK and Caspase Inhibitors on BzATP-induced IL-1β release. The differentiated THP-1 cells were pretreated for 30 minutes with 10 μM of the listed MAPK inhibitors , caspase inhibitors, and control compounds prior to stimulation of IL-1β release with 1 mM BzATP. Data are shown as a percentage of BzATP induced IL-1β release in the absence of inhibitors (which usually ranged from 200-600 pg/ml of IL-1β). Values shown represent the means ± S.E.M. of 3-5 experiments in duplicates. Statistical significance (*) represents a difference between control and experimental values with the use of analysis of variance (ANOVA) and * denotes P<0.05 and ** denotes P < 0.01.

Figure 8. Concentration effect curves for a caspase 1 inhibitor, YVAD and a caspase 3 inhibitor, DEVD, to attenuate 1 mM BzATP induced IL-1β release (which ranged from 200-600 pg/ml) Results are shown as a percentage of BzATP induced IL-1β release in the absence of inhibitors. Data represent mean ± S.E.M. of 3-5 experiments.

Figure 9. Yo-Pro uptake stimulated by MTX in LPS/IFNγ differentiated THP-1 cells or ATP in $P2X_{2a}R$ expressing 1321N1 cells. A. Concentration effect curve for MTX to induce Yo-Pro uptake in LPS/IFNγ differentiated THP-1 cells. Data were normalized to the peak BzATP response (% Response). B. Concentration-effect curve for inhibition of MTX (10 pM)-induced Yo-Pro uptake by calmidazolium. C. Concentration-effect curve for ATP to induce Yo-Pro uptake in $P2X_{2a}R$ expressing 1321N1 cells (Lynch et al., 1999). B) Concentration effect response of ATP to induce pore formation in 1321 cells expressing the $hP2X_{2a}$ receptors. Data were normalized to the peak ATP response (% Maximum Response). D. Concentration-effect curve for inhibition of ATP (10 μM)-induced Yo-Pro uptake by PPADS. All data represent mean ± S.E.M. of 3-5 experiments.

JPET Fast Forward. Published on November 21, 2003 as DOI: 10.1124/jpet.103.059600
This article has not been copyedited and formatted. The final version may differ from this version.

Table I: *Effects of MAPK and Caspase Inhibitors on 50 μM BzATP-Induced Yo-Pro Uptake in Differentiated THP-1 Cells.*

Compound	**IC_{50} (nM)**	**n**
MAPK Inhibitors:		
SB 202190	75 ± 6	6
PD 169316	1600 ±412	4
SB 203580	9734 ± 876	5
SB 202474	>100000	3
PD 98059	> 30000	3
U0126	>100000	3
5-Iodotubercidin	>100000	3
Caspase Inhibitors:		
YVAD, capsase 1	8000 ± 800	4
DEVD, caspase 3	3200 ± 300	4
Cathepsin B, (-) Control	>30000	3
Dynorphin A, control peptide	>30000	3
Oxytocin, control peptide	>30000	3

JPET Fast Forward. Published on November 21, 2003 as DOI: 10.1124/jpet.103.059600
This article has not been copyedited and formatted. The final version may differ from this version.

Table II: *Effects of Inhibitors of PKC and intracellular calcium modulators on 50 μM BzATP-Evoked Yo-Pro Uptake in THP-1 Cells*

Compound	**IC_{50} (μM)**	**n**
Thapsigargin	>100	3
Xestospongin C	>100	3
Go- 6976	4.9 ± 0.6	4
Ro-31-7549	2.5 ± 0.1	4
Ro-31-8220	2.4 ± 0.1	6

JPET Fast Forward. Published on November 21, 2003 as DOI: 10.1124/jpet.103.059600
This article has not been copyedited and formatted. The final version may differ from this version.

Table III . *Differential Mechanisms of Yo-Pro Uptake.*

	THP-1	**1321-hP2X$_{2a}$**	**THP-1**
Pore Stimulus	**50 μM BzATP***	**10 μM ATP***	**10 pM MTX****
Compound:	**IC$_{50}$ (μM)**		
PPADS	0.334 ± 0.017	0.477 ± 0.012	>100
KN-62	0.044 ± 0.002	>100	>100
Calmidazolium	>100	>100	7.9 ± 0.2
U73122	>100	>100	1.8 ± 0.4
SB 202190	0.075 ± 0.006	>100	>100
DEVD, caspase 3	3.2 ± 0.3	7.2 ± 0.5	>100

* Denotes assay buffer were both Ca^{++} and Mg^{++} free.
** Denotes assay buffer contained both Ca^{++} and Mg^{++}.

JPET Fast Forward. Published on November 21, 2003 as DOI: 10.1124/jpet.103.059600
This article has not been copyedited and formatted. The final version may differ from this version.

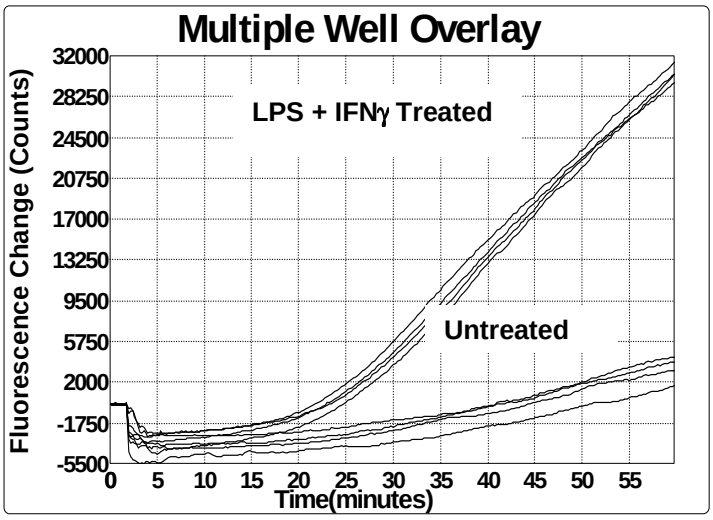

A

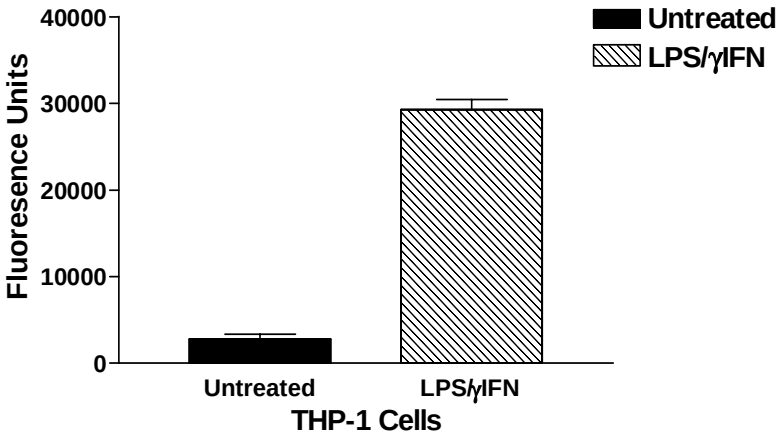

B

JPET Fast Forward. Published on November 21, 2003 as DOI: 10.1124/jpet.103.059600
This article has not been copyedited and formatted. The final version may differ from this version.

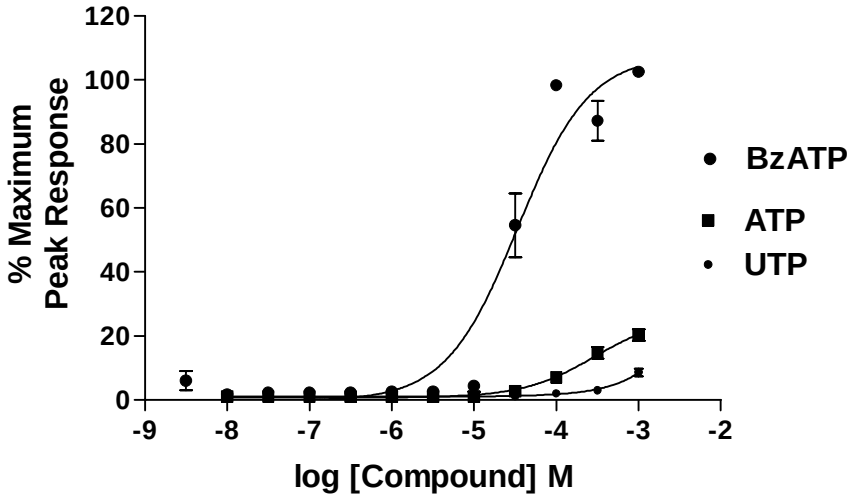

A

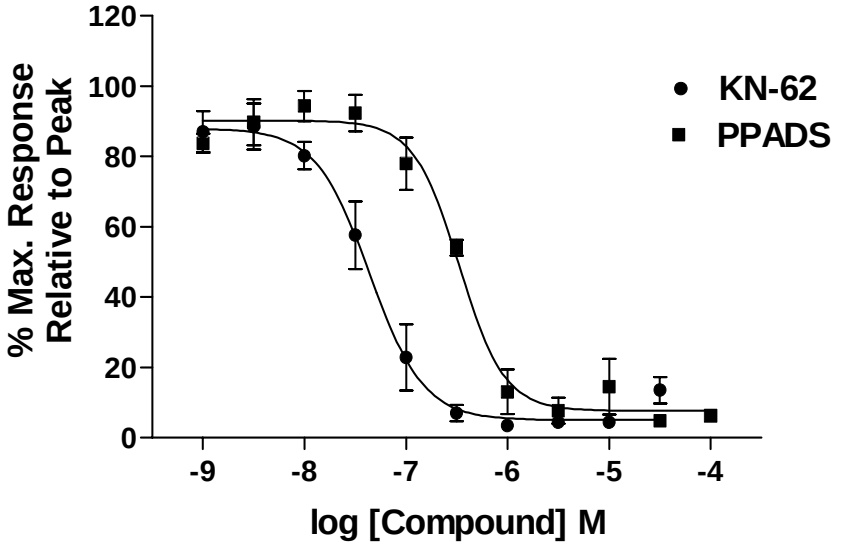

B

JPET Fast Forward. Published on November 21, 2003 as DOI: 10.1124/jpet.103.059600
This article has not been copyedited and formatted. The final version may differ from this version.

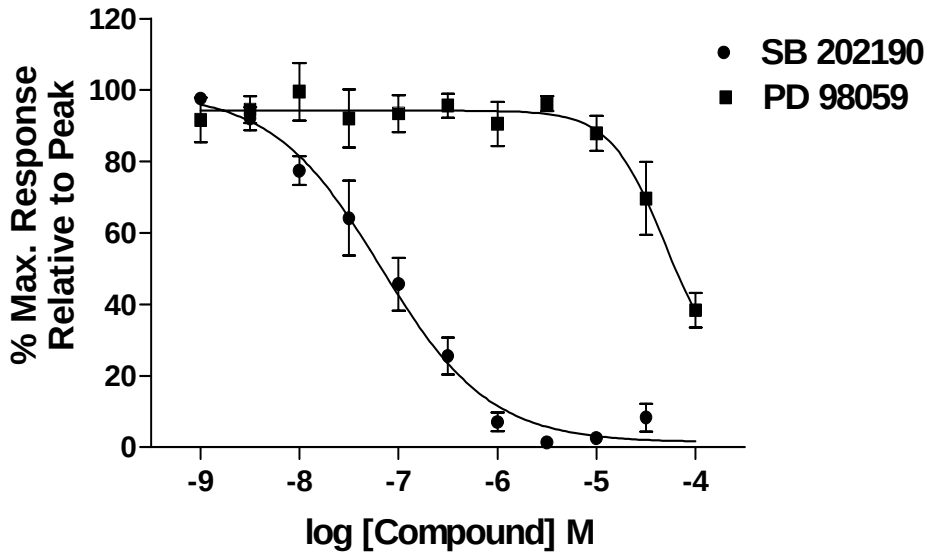

JPET Fast Forward. Published on November 21, 2003 as DOI: 10.1124/jpet.103.059600
This article has not been copyedited and formatted. The final version may differ from this version.

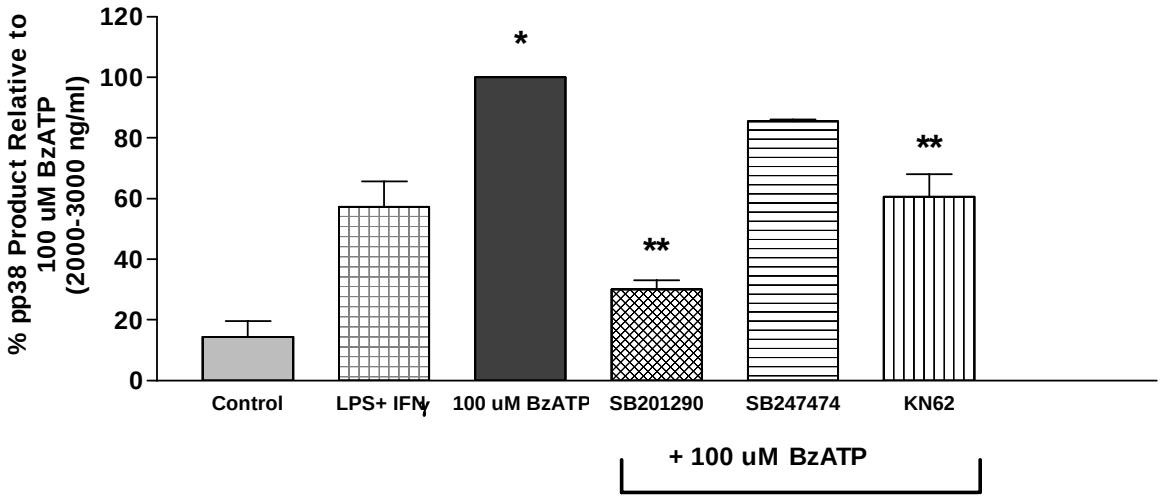

JPET Fast Forward. Published on November 21, 2003 as DOI: 10.1124/jpet.103.059600
This article has not been copyedited and formatted. The final version may differ from this version.

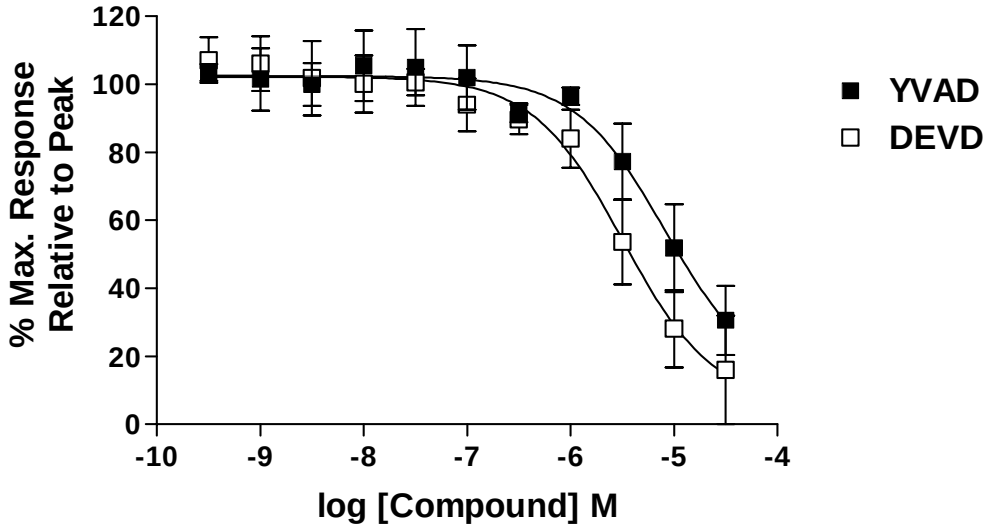

JPET Fast Forward. Published on November 21, 2003 as DOI: 10.1124/jpet.103.059600
This article has not been copyedited and formatted. The final version may differ from this version.

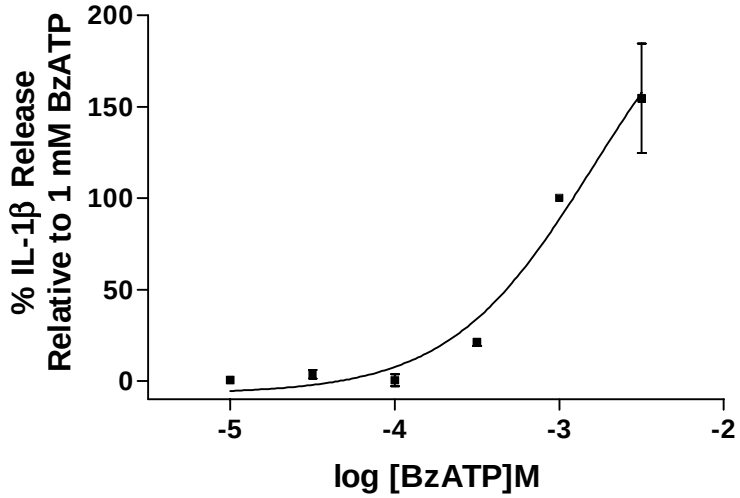

A

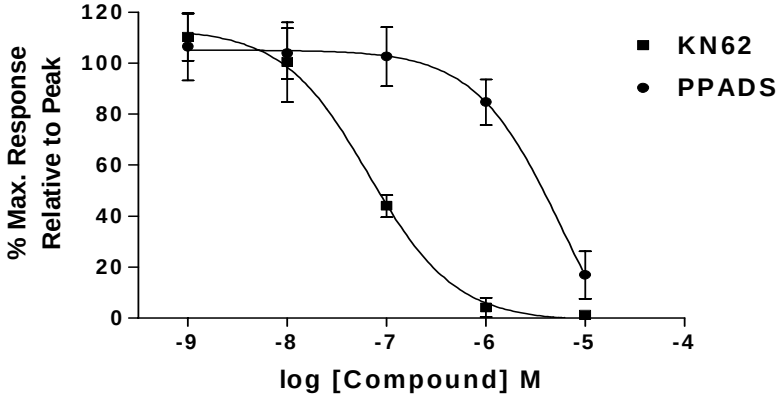

B

JPET Fast Forward. Published on November 21, 2003 as DOI: 10.1124/jpet.103.059600
This article has not been copyedited and formatted. The final version may differ from this version.

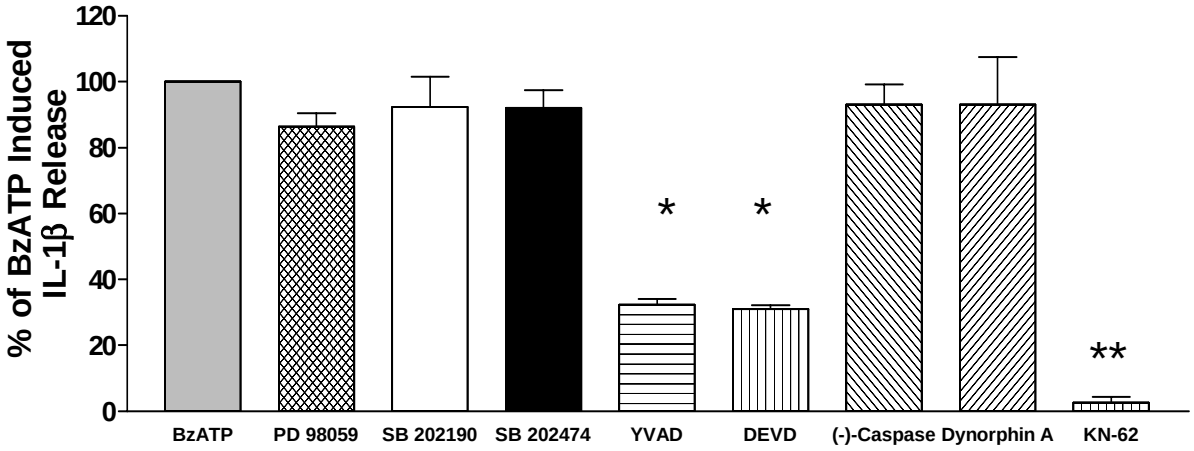

JPET Fast Forward. Published on November 21, 2003 as DOI: 10.1124/jpet.103.059600
This article has not been copyedited and formatted. The final version may differ from this version.

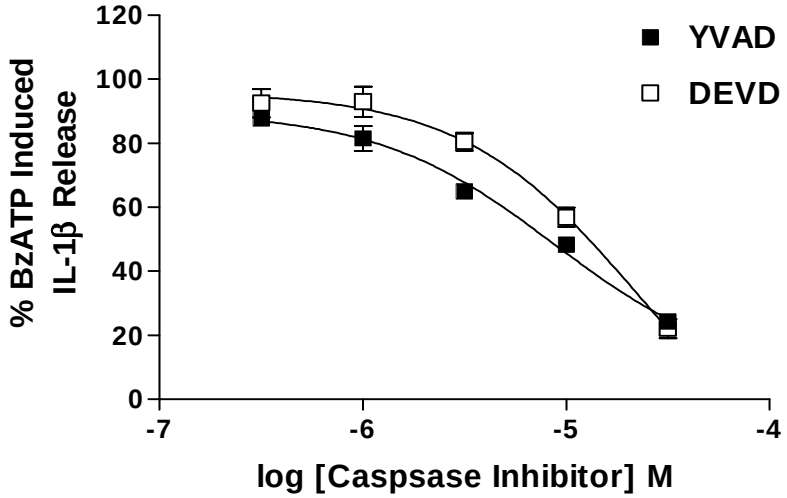

JPET Fast Forward. Published on November 21, 2003 as DOI: 10.1124/jpet.103.059600
This article has not been copyedited and formatted. The final version may differ from this version.

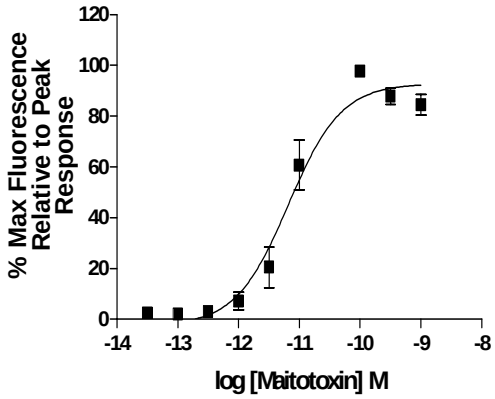

A

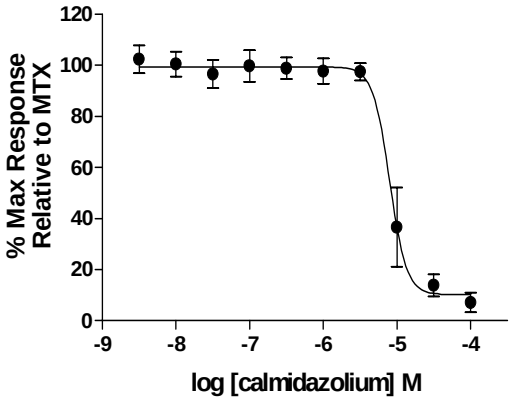

B

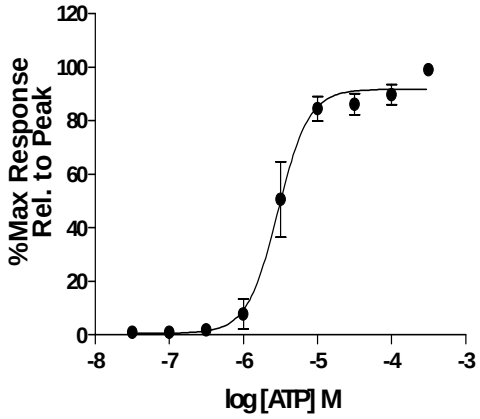

C

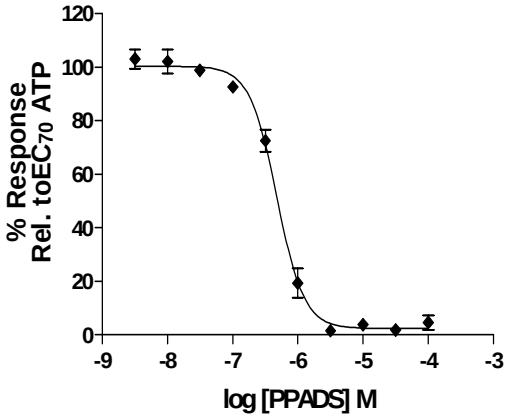

D